J. Braz. Chem. Soc., Vol. 13, No. 5, 611-617, 2002.
Printed in Brazil - ©2002 Sociedade Brasileira de Química
0103 - 5053 $6.00+0.00

Article

Antimony (V) Oxide Adsorbed on a Silica-Zirconia Mixed Oxide Obtained by the Sol-Gel Processing Method: Preparation and Acid Properties

Galina Zaitseva[b] *and Yoshitaka Gushikem*[*,a]

[a] *Instituto de Química, Universidade Estadual de Campinas, CP 6154, 13083-970 Campinas - SP, Brazil*

[b] *Institute of Sorption and Endoecology Problems, Kiev, 252680 Ukraine*

A preparação, o grau de dispersão, estabilidade térmica e a acidez de Lewis e de Brϕnsted do óxido de antimônio (V) adsorvido sobre SiO_2/ZrO_2, preparado previamente pelo processo sol-gel, são descritas neste trabalho. Amostras de $SiO_2/ZrO_2/Sb_2O_5$ de composições (% em massa): (a) Zr= 8,1 e Sb= 6,3; (b) Zr= 11,4 e Sb= 11,4, foram preparadas. As imagens de microscopia eletrônica de varredura conectada a um espectrômetro de energia dispersiva de raios X mostraram que os metais, Zr e Sb, estão homogeneamente dispersos em ambas as matrizes. Os padrões de difração de raios X de $SiO_2/ZrO_2/Sb_2O_5$ aquecido a diversas temperaturas mostraram que até 1023 K a amostra apresentou-se amorfa. Em 1273 K a formação da fase cristalina ZrO_2 (baddeleita) foi observada e elevando-se a temperatura a 1573 K, as fases cristalinas de SiO_2 (cristobalita) e possivelmente de ZrO_2/Sb_2O_5 foram observadas. Utilizando a piridina como sonda molecular, sítios ácidos de Brϕnsted do sólido $SiO_2/ZrO_2/Sb_2O_5$, aquecido até 523 K, mostraram ser bastante estáveis.

The preparation, degree of dispersion, thermal stability and Lewis and Brfnsted acidity of antimony (V) oxide adsorbed on SiO_2/ZrO_2 mixed oxide, previously prepared by the sol-gel processing method, are described herein. The samples $SiO_2/ZrO_2/Sb_2O_5$, with compositions (in wt %): (a) Zr= 8.1 and Sb= 6.3; (b) Zr= 14.9 and Sb= 11.4, were prepared. Scanning electron microscopy images connected to a X-ray energy dispersive spectrometer showed that both metals, Zr and Sb, were highly dispersed in the matrices. The X-ray diffraction patterns of $SiO_2/ZrO_2/Sb_2O_5$ heated at different temperatures showed that, up to 1023 K, the matrix was amorphous. At 1273 K a crystalline phase of ZrO_2 (baddeleyite) was observed and raising the temperature to 1573 K, crystalline phases of SiO_2 (cristobalite) and presumably of ZrO_2/Sb_2O_5 were observed. Using pyridine as a molecular probe, Brϕnsted acid sites on the $SiO_2/ZrO_2/Sb_2O_5$ matrix, heat treated up to 523 K, were shown to be very stable.

Keywords: sol-gel method, silica-zirconia-antimony mixed oxide, Brϕnsted and Lewis acid sites

Introduction

Antimony oxide, Sb_2O_5, as amorphous or crystalline phases, is normally obtained as a fine powder presenting low mechanical and thermal resistance.[1,2] limiting its use when a rigid and porous matrix is required. Since the oxide presents good acid properties and to overcome this problem, Sb_2O_5 has been obtained in a highly dispersed form by the grafting reaction of $SbCl_5$ on a SiO_2 surface from a non aqueous solvent.[3] The material obtained SiO_2/Sb_2O_5, combined the acid properties of the antimony oxide with the mechanical and thermal resistance of the SiO_2 matrix. The oxide is attached to the surface by Si-O-Sb bond formation.[3] However, the use of the material has been limited to neutral aqueous solutions because antimony oxide is leached off the surface, due to the easy hydrolysis of the Si-O-Sb bond in acid solution.

An alternative way to obtain chemically stable Sb_2O_5 is to adsorb Sb(V) on a binary mixed oxide matrix obtained by the sol-gel processing method.[4] This procedure has been used in order to obtain Sb_2O_5 dispersed on a SiO_2/TiO_2 matrix, rendering the antimony oxide practically insoluble in an acid solution due to the formation of the new titanium (IV) antimonate phase.

The use of the mixed oxide prepared by the sol-gel method is very important because it permits to obtain a

* e-mail: gushikem@iqm.unicamp.br

material where the components are highly and homogeneously dispersed in the matrix.[5-13] This work describes the procedure to adsorb antimony (V) oxide on SiO_2/ZrO_2, previously obtained by the sol-gel processing method, aiming to obtain a homogeneous and poorly soluble zirconium oxide-antimoium oxide phase immobilized on the SiO_2 surface. The physical properties of the material, obtained by X-ray diffraction (XRD), X-ray photoelectron spectroscopy (XPS), and scanning electron microscopy (SEM) connected to a X-ray emission analyzer are described. The thermal stability of the Brϕnsted solid acid, by using pyridine as the molecular probe, is also described.

Experimental

Preparation of SiO_2/ZrO_2 by the sol gel method

The silica-zirconia mixed oxides, containing two different compositions of the metal oxide, were prepared by the sol gel method as described elsewhere, with some modifications.[14] In a reaction flask containing 250 mL of tetraethylorthosilicate (TEOS, Aldrich; 1.1 mol), 14 mL of aqueous HCl 3 mol L^{-1} solution were carefully added and the resulting solution was stirred for 3 h at 333 K. A solution containing 28 mL of zirconium tetrabutoxide ($ZrBu_4$, Aldrich; 0.061 mol) in 80 mL of dry ethanol was slowly added under an argon atmosphere and the mixture was stirred for 1.5 h. In a second preparation, a mixture containing 69 mL of $ZrBu_4$ (0.15 mol) and 80 mL of dry ethanol was used. About 7 mL of 3 mol L^{-1} HCl solution was added dropwise in the first preparation and 17.5 mL of 3 mol L^{-1} HCl solution in the second one. The resulting mixtures were allowed to rest for 16 h. The solvents were evaporated by gently heating the mixture at 353 K. The xerogel formed in each preparation was ground and sieved between 200-250 mesh, washed with ethanol in a soxhlet apparatus and then immersed in 0.1 mol L^{-1} HCl solution for 24 h, filtered and dried under vacuum at 333 K.

Reaction of SiO_2/ZrO_2 with Sb(V)

About 20 g of SiO_2/ZrO_2 xerogel was immersed in 50 mL of an acid solution (2.5 mol L^{-1} HCl) of 0.45 mol L^{-1} Sb(V). The volume was completed to 800 mL with pure water and the mixture was stirred at 333 K for 7h. The solid was filtered, washed with water until the filtrate solution was neutral, and dried at 333 K in an oven.

Chemical analyses

Samples of about 0.1 g of SiO_2/ZrO_2 or $SiO_2/ZrO_2/Sb_2O_5$ were treated with a few drops of 40% HF solution (v/v) until complete dissolution of the solid. HF was eliminated from the solution with a HNO_3:HCl mixture (1:15 v/v) and the Sb and Zr contents were analyzed using atomic absorption spectroscopy on a Perkin Elmer Optima 3000 DV apparatus.

Physical measurements

The scanning electron micrograph images were obtained from a JEOL JSM T-300 microscope by dispersing the sample on a conducting double-faced tape adhered to an aluminum support. The adhered samples were coated with a thin film of graphite by using the low voltage sputtering technique on a Plasma Science Model LVC 76 apparatus. The X-ray emission analysis was made using a Tracor Northern EDS microprobe.

UV-Visible diffuse reflectance spectra (DRS)

UV-Vis DRS spectra of the samples were obtained by using a UV-VIS-NIR Cary 5G spectrophotometer. The measurements were carried out using $BaSO_4$ as the blank reference.

X-ray photoelectron spectroscopy (XPS) spectra of the samples were obtained by using an aluminum anode (AlK_α=1486.6 eV) at a pressure of $2.66´10^{-5}$ Pa on a McPherson ESCA-36 spectrometer. The atomic ratios were estimated by integrating the areas under the peaks using the corresponding Scofileld cross section[15] for each atomic level involved. The binding energies were calibrated against C1s at 284.6 eV.

X-ray diffraction patterns were obtained using Cu$K\alpha$ radiation (λ = 0.154 nm) at 30 kV, current of 20 mA and a scan rate of 0.033^0 s^{-1} (degree in 2θ) on a Shimadzu 600 diffractometer.

Specific surface area (S_{BET}) was determined by the BET method by using an ASAP 2010 apparatus from Micromeritics.

The nature of surface acid sites was determined by using pyridine as a molecular probe. Self-supported pressed disks of the sample were previously degassed at 353 K under vacuum and impregnated with pyridine molecules. The transmission IR spectra were obtained for samples previously heat treated under vacuum at 298, 323, 423 and 473 K. The spectra were recorded at room temperature after 100 cumulative scans with 4 cm^{-1} resolution. The measurements were carried out on a Bomem MB series spectrophotometer.

Results and discussions

Table 1 presents the results of the chemical analyses of the samples. The amounts of Zr(IV) loading in the two

Table 1. Results of the chemical analyses and specific surface areas for SiO_2/ZrO_2 and $SiO_2/ZrO_2/Sb_2O_5$

Samples	Zr/wt %	Sb/wt %	S_{BET} /m^2 g^{-1}	Aver. Pore Diameter/nm
SiO_2/ZrO_2 (I)	8.4 (0.92)	-	-	-
SiO_2/ZrO_2 (II)	15.4 (1.68)	-	-	-
$SiO_2/ZrO_2/Sb_2O_5$ (I)	8.1 (0.89)	6.3 (0.52)	590	0.73
$SiO_2/ZrO_2/Sb_2O_5$ (II)	14.9 (1.64)	11.4 (0.93)	440	0.69

( ): mmol of the metal per gram of the matrix.

matrices are 8.4 and 15.4 wt%, corresponding to 0.92 and 1.68 mmol g^{-1} (amount of zirconium per gram of the sample), respectively. These samples will hereafter be designated as SiO_2/ZrO_2(I) and SiO_2/ZrO_2(II), for the first and second samples, respectively. Incorporation of Sb(V) on these two matrices were 6.3 and 11.4 wt% or 0.52 and 0.93 mmol g^{-1}, respectively. These two samples will be hereafter designated as $SiO_2/ZrO_2/Sb_2O_5$(I) and $SiO_2/ZrO_2/Sb_2O_5$(II). The Sb/Zr mol ratios in both samples are nearly the same, 0.58 and 0.57, respectively. These values suggest that incorporation of Sb(V) onto the SiO_2/ZrO_2 matrices arises from the interaction of the metal ion with the surface Zr(IV). We may suppose that the reaction can be described by the following reaction:

$$n\equiv ZrOH + Sb(OH)_5 \rightarrow (\equiv ZrO)_n Sb(OH)_{5-n} + nH_2O \qquad (1)$$

where ≡ZrOH stands for hydrated zirconium oxide bonded to the SiO_2 surface. This supposition is strongly supported by the fact that Sb(V) does not form stable Si-O-Sb bonds with ≡SiOH on the SiO_2 surface at low pH, since it is easily hydrolyzed.[3] The solubility of Sb(V) in acid solution was negligible, ~10^{-6} mol per gram of the material, determined by shaking the $SiO_2/ZrO_2/Sb_2O_5$ samples in 0.1 mol L^{-1} HCl solution for 24 h at 298 K.

The specific surface area, S_{BET}, for $SiO_2/ZrO_2/Sb_2O_5$ is smaller for the sample with the higher amount of antimony loading, 590 m^{2}g^{-1} for (I) and 440 m^{2}g^{-1} for (II) and the average pore diameters are 0.73 and 0.69 nm, respectively.

UV-vis DRS

The UV-vis DRS spectra of SiO_2/ZrO_2 and $SiO_2/ZrO_2/Sb_2O_5$ samples are shown in Figure 1. The band maxima for SiO_2/ZrO_2 for the samples with 8.4 wt% (Figure 1b) and 15.4 wt% (Figure 1a) loadings of ZrO_2 are observed in both cases at near 228 nm, which correspond to the oxygen to metal charge transfer transition of Zr(IV). Upon Sb(V) loading, the band maxima shift to the higher energy region, near 200 nm (Figures 1c and 1d). For bulk phase ZrO_2, this band maximum is observed between 230-240 nm.[16,17] The band shift to a lower wavelength region is normally

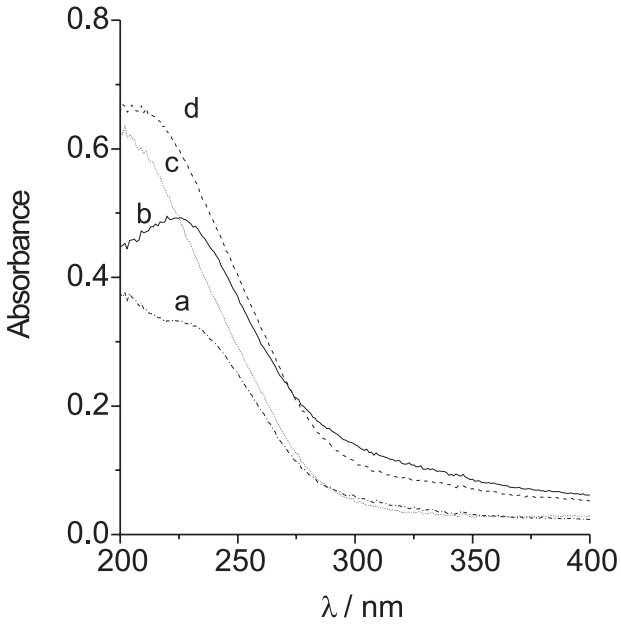

Figure 1. UV-vis DRS of: (a) SiO_2/ZrO_2 (II); (b) SiO_2/ZrO_2 (I); (c) $SiO_2/ZrO_2/Sb_2O_5$ (II); (d) $SiO_2/ZrO_2/Sb_2O_5$ (I).

associated with a high dispersion of Zr(IV) in the matrices, with formation of smaller particles. This may occur, in our case, due to the reaction of the immobilized Zr(IV) with Sb(V), as described in reaction (1), resulting a new highly dispersed zirconium-antimonate phase.

XPS results

Table 2 lists the binding energy (BE) values and the atomic ratios of interest. The $Zr3d_{5/2}$ BE are observed at *ca.* 183 eV in SiO_2/ZrO_2 and $SiO_2/ZrO_2/Sb_2O_5$, a value which is slightly higher than that for bulk ZrO_2, observed at 182.2 eV.[18] This increase of the BE is related with stronger Zr-O bond polarization[19] due to the interaction of Zr with both the surface ≡SiOH and with Sb(V). For both samples the $Sb3d_{3/2}$ BE, in comparison with that of bulk phase Sb_2O_5 observed at 540.2 eV,[20] did not show any significant change. On the surface, at the depth distance probed by XPS, the Zr/Si atomic ratios are 0.088 and 0.21 for SiO_2/ZrO_2 (I) and (II), respectively. These values roughly agree with the

Table 2. Binding Energies (in eV) for SiO_2/ZrO_2 and $SiO_2/ZrO_2/Sb_2O_5$

Samples	$Sb3d_{3/2}$	$Zr3d_{5/2}$	Si2p	Zr/Si*	Sb/Si*
SiO_2/ZrO_2(I)		183.0	102.9		
SiO_2/ZrO_2(II)		183.0	102.8		
$SiO_2/ZrO_2/Sb_2O_5$ (I)	540.1	182.8	103.2	0.074	0.23
$SiO_2/ZrO_2/Sb_2O_5$ (II)	539.8	183.0	102.6	0.27	0.25
SiO_2			103.3		
ZrO_2[a]		182.2			
Sb_2O_5[b]	540.2				

* Zr/Si and Sb/Si atomic ratios were determined from the ratios of integrated areas under BE peaks of the elements; [a] reference 22; [b] reference 20.

$ZrBu_4$/TEOS molar ratios used for preparation of the samples, 0.061 and 0.14. This correspondence suggests that Zr(IV) oxide is highly and homogeneously dispersed in both matrices. The Sb/Si atomic ratios, for both $SiO_2/ZrO_2/Sb_2O_5$, are practically the same, *i.e.* 0.23 and 0.25.

Electron micrographs

Figure 2a shows the scanning electron microscopy (SEM) image of the $SiO_2/ZrO_2/Sb_2O_5$ with the higher antimony loading and Figures 2b and 2c the corresponding EDS images. The white points in Figures 2b and 2c are due to the metal emission lines ZrKα = 2.05 keV and SbLα = 3.6 keV,[21] respectively. The SEM and EDS images show that, within the magnification used, the zirconium (IV) and antimony (V) oxide particles are homogeneously dispersed in the matrices with no detectable segregated phases.

X-ray diffraction

Table 3 lists the main X-ray diffraction peaks (intesities higher than 10) of standard SiO_2 (cristobalite)[22,23]; ZrO_2 baddeleyite[22] and Sb_2O_5[22] and the observed peaks for $SiO_2/$

Table 3. Selected X-ray diffraction peaks of standard samples[8] and those observed for $SiO_2/ZrO_2/Sb_2O_5$

SiO_2[a]		ZrO_2[b]		Sb_2O_5[c]		$SiO_2/ZrO_2/Sb_2O_5$	
2θ	Int	2θ	Int	2θ	Int	2θ	Int
				14.9	25		
21.9	100					21.9	20
		28.2	100			28.3	60
				28.7	20		
				30.0	100	30.3	100
		31.5	68			31.4	20
				34.4	11	34.6	15
		35.3	13			35.4	17
						50.0	70
				50.0	25		
		50.2	22				
				59.5	30		
						60.2	40

*Only peaks having intensities greater than 10 are listed. ref. 22[a,b,c].

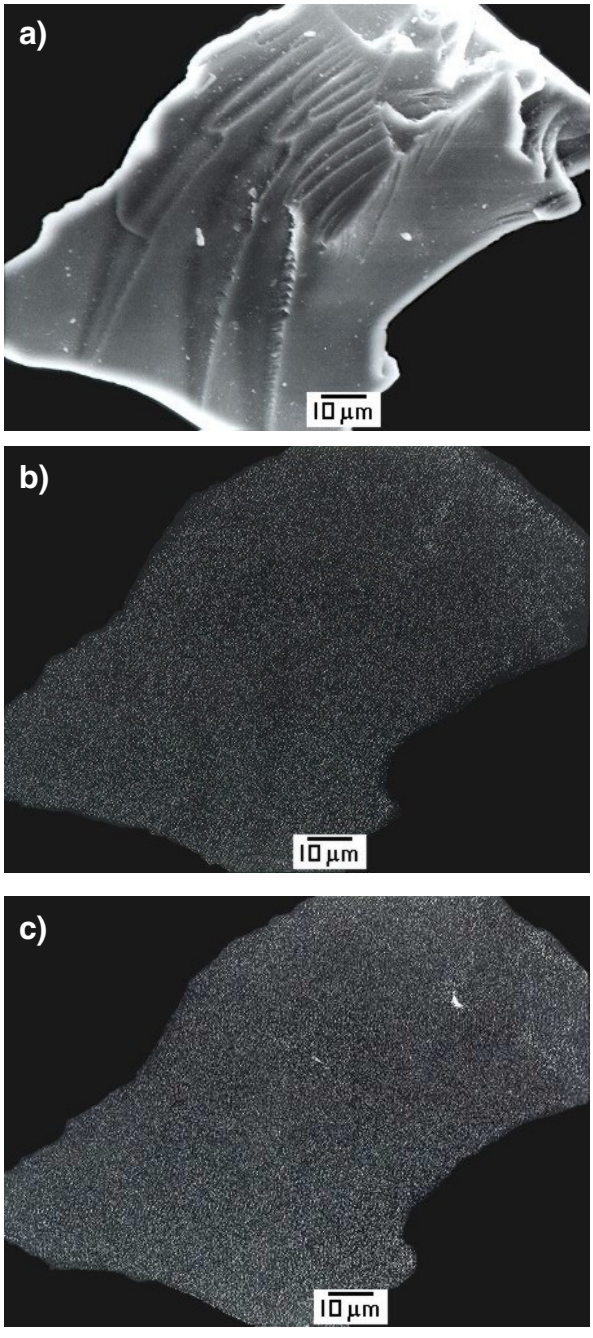

Figure 2. (a) SEM image of $SiO_2/ZrO_2/Sb_2O_5$ (II); The corresponding EDS images for (b) Zr mapping and (c) Sb mapping.

ZrO_2/Sb_2O_5. Figures 3a to 3d shows the XRD patterns for $SiO_2/ZrO_2/Sb_2O_5$ samples heat treated from 773 up to 1573 K. For the material heated at 773 (3a) and 1023 K (3b), the absence of diffraction peaks indicates that the material is amorphous. At 1273 K (3c) the process of sample crystallization is observed. Increasing the temperature up to 1573 K, the crystallization process is completed. The peak at 30.3 (100), where the number in parenthesis is the relative intensity, is assigned to Sb_2O_5 because ZrO_2 crystalline species (Table 3) does not show any peaks in this region. The most intense peak of ZrO_2 is observed at 28.2^0 (100), and in $SiO_2/ZrO_2/Sb_2O_5$ it appears at 28.3 (60). For the bulk phase, a standard antimony oxide peak is observed at 28.7 (20) but, in this case, its intensity is considerably lower. The diffraction peak of antimony oxide (Figure 3e) at 14.8^0, despite its intensity, is not observed in Figure 3d. The peak observed at 21.9^0 in Figure 3e is due to the SiO_2 as cristoballite (see Table 3), indicating that this phase is segregated for samples heat treated at 1573 K. The peak at 60.2^0 (40) in Figure 3d is not observed in antimony oxide or in zirconium oxide phases (see Table 3). This last peak is unequivocally assigned to a different phase, presumably formed by the reaction between Sb(V) and Zr(IV) on the matrix surface, but unfortunately, the structure of this phase is unknown.[24]

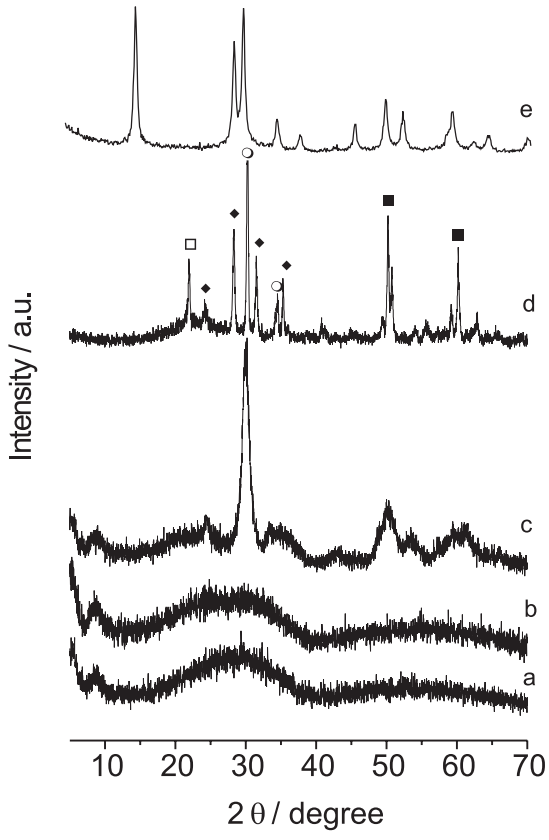

Figure 3. XRD patterns for $SiO_2/ZrO_2/Sb_2O_5$ (II) heat treated at various temperatures: a) 773 K, b) 1023 K, c) 1273 K, d) 1573 K (□ SiO_2; ◆ ZrO_2; ○ Sb_2O_5; ■ zirconium oxide-antimonium oxide new phase) and e) for Sb_2O_5 crystalline phase.

Acid properties

Figure 4 shows the IR spectra of pyridine adsorbed on $SiO_2/ZrO_2/Sb_2O_5$(I) heat treated at various temperatures from 323 to 573 K. Four vibrational modes assignable to the pyridine molecule are shown. The absorption band at 1445 cm^{-1}, whose intensity changes for the sample heat treated at higher temperatures and practically disappears at 573 K, is assigned to the 19b mode of pyridine, attached by hydrogen bonds to unreacted ≡SiOH groups.[3,25] The band at 1457 cm^{-1}, which appears as a shoulder at 373 K and is clearly observable for sample heated at 573 K, is assigned to the pyridine 19b mode bonded to a Lewis acid site (LAS).[26] This LAS is mainly due to the highly dispersed coordinatively unsaturated Sb(V) on the surface. For sample $SiO_2/ZrO_2/Sb_2O_5$(I), the XPS technique shows that atomic ratio Sb/Zr ~ 3 (calculated from data of Table 2) and taking into account the depth the technique can probe (about 30 nm in the present case), we can consider that at the matrix surface the concentration of antimony is nearly three times higher compared to zirconium. For chemical evidence that this assumption is correct, Alizarine Red S (AlizRS) dye was adsorbed from aqueous solution onto SiO_2/ZrO_2(I) and $SiO_2/ZrO_2/Sb_2O_5$(I) surfaces (Figure 5). It is well known that this reagent reacts with hydrated ZrO_2

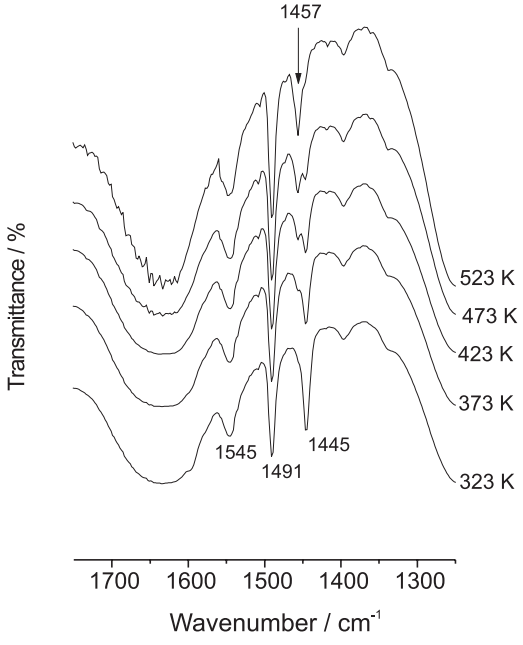

Figure 4. FT IR spectra of pyridine molecules adsorbed on $SiO_2/ZrO_2/Sb_2O_5$ (I) heat treated at various temperatures.

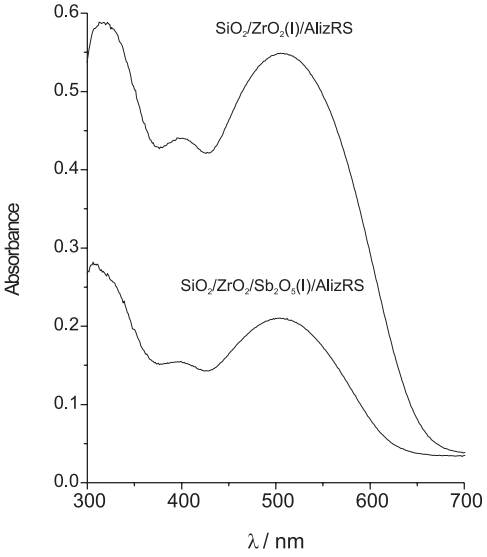

Figure 5. UV-vis DRS of Alizarin Red S adsorbed on SiO_2/ZrO_2 (I) and $SiO_2/ZrO_2/Sb_2O_5$ (I).

forming a 1:1 Zr/AlizRS complex whose maximum is observed as a broad band at about 500 nm (it is important to mention that Sb(V) and SiO_2 do not react with AlizRS).[27] The intensity of this band is considerably reduced, about 1/3 for $SiO_2/ZrO_2/Sb_2O_5$(I) in comparison with SiO_2/ZrO_2(I). As the bulk Sb_2O_5 and SiO_2 do not present LAS[3,28] the band at 1457 cm^{-1} in Figure 4 is mainly due to LAS on coordenatively unsaturated Sb(V) on the $SiO_2/ZrO_2/Sb_2O_5$(I) surface.

The band observed at 1491 cm^{-1} is the pyridine 19a mode and, practically, does not shift when sorbed in different sites.[29] The band observed at 1545 cm^{-1} is due to the 19b mode of the pyridinium ion adsorbed on Brϕnsted acid sites (BAS).[24,30] It is very important to observe that the band intensity of this mode remains unchanged even for a sample treated at 573 K. For bulk Sb_2O_5, this band is not observed for samples heat treated at this temperature, because the solid easily dehydrates and the BAS disappear.

Conclusions

SiO_2/ZrO_2 mixed oxide obtained by a sol-gel processing method adsorbs Sb(V) from acid solution forming a phase, not characterized, on the matrix surface. The materials obtained, $SiO_2/ZrO_2/Sb_2O_5$, have high surface areas, 590 and 440 $m^2\ g^{-1}$ for the samples with lower and higher antimony contents, respectively. The Brϕnsted acid sites are thermally very stable, being observed for samples heated up to 573 K. This thermal stability results from the low surface density, $\delta = N_o x N/S_{BET}$, where N_o and N are the amount of the zirconium-antimony oxide phase and Avogadro's number, respectively. Assuming that zirconium-antimony particles are homogeneously dispersed on the matrix the average inter-atomic distance, l_{ij}, can be estimated[23] by applying the equation $l_{ij} = (1/\delta)^{1/2}$. The estimated values are *ca.* 1.2 and 0.7 nm for $SiO_2/ZrO_2/Sb_2O_5$(I) and $SiO_2/ZrO_2/Sb_2O_5$(II), respectively. With these low surface densities of the zironium-antimony oxide particles on the matrix surface, the tendency of collapse into larger ones, with intermolecular loss of water and, consequently, reduction of the BAS and LAS on the surface, is minimized.[19]

Acknowledgements

G.Z. is indebted to Fundação de Amparo a Pesquisa do Estado de São Paulo (FAPESP), Brazil, for a Post-Doctoral fellowship and Y.G. to FAPESP and FINEP/Pronex for financial support. English revision by Prof. Carol H. Collins is also acknowledged.

References

1. Abe M.; Ito T.; *Bull. Chem. Soc. Jpn*. **1968**, *41*, 2366.
2. Abe M.; Chitrakar R.; Tsuji M.; Fukumoto K.; *Solv. Extr. Ion Exch*. **1985,** *3*, 149.
3. Benvenutti, E.V.; Gushikem, Y.; Davanzo, C.U.; C. de Castro, Sandra; Torriani, I.L.; *J. Chem. Soc., Faraday Trans*. **1992**, *88*, 3193.
4. Gonçalves, J.E.; Gushikem, Y.; de Castro, S.C.; *J. Non-Cryst. Solids* **1999**, *260*, 125.
5. Salvado, M.J.M.; Margaça, F.M.A.; Teixeira, J.; *J. Non-Cryst. Solids* **1993**, *163*, 115.
6. De Lange, R.S.A.; Kleizer, J.H.A.; Burgraaf,; A.J.; *J. Non-Cryst. Solids* **1995**, *191*, 1.
7. Haereid, S.; Dahle, M.; Lima, S.; Einarsud, M.A.; *J. Non-Cryst. Solids* **1995**, *186*, 96.
8. Alfaya, A.A.S.; Gushikem Y.; *J. Colloid Interface Sci*. **1999**, *209*, 428.
9. Turner, M.R.; Duguet, E.; Labrugere, C.; *Surf. Interface Anal*. **1997**, *25*, 917.
10. Toba, M.; Mizukami, F.; Niva, S.; Sato, T.; Maeda, K.; Annila, A.; Komppa, V.; *J. Mol. Catal*. **1994** *,94*, 85.
11. Anderson J.A.; Fergusson C.; Rodriges-Ramos, I.; Guerrero-Ruiz, A.; *J.Catal*. **2000**, *192*, 344.
12. de Monte, F.; Larsen, W.; Mackenzie, J.D.; *J. Am. Ceram. Soc*. **2000**, *83*, 1506.
13. Pickup, D.M.; Mountjoy G.; Wallidge, G.W.; Newport, R.J.; Smith, M.E.; *Phys. Chem. Chem. Phys*. **1999**, *1*, 2527.
14. Alfaya, A.A.S.; Gushikem, Y.; de Castro, S.C.; *Micr. Mesop. Mater*. **2000**, *39*, 57.

15. Scofield, J.H.; *J. Electron Spectrosc. Relat. Phenom*. **1976**, *8*, 129.
16. Gao X.; Fierro, J.L.G. ; Wachs, I.E.; *Langmuir* **1999**,*15*, 3169.
17. Moon, S.C.; Fujino, M.; Yamashita H.; Anpo, M.; *J. Phys. Chem. B* **1997**, *101*, 369.
18. *Handbook of Photoelectron Spectroscopy*; Perkin-Elmer, Eden Praine, 1992
19. Alberti, G.; Costantino, U.; Marletta, G.; Puglisi, O.; Pignataro; S.; *J. Inorg. Nucl. Chem.* **1981**, *43*, 3329.
20. Morgan, W.E.; Stec, W.J.; Van Wazer, J.R.; *Inorg. Chem*. **1973**, *12*, 953.
21. Goodhew P.J.; Humphreys, F.J.; *Electron Microscopy and Analysis*, 2nd ed., Taylor and Francis: London, 1992.
22. *Powder Diffraction File Search Manual, The Joint Committee on Powder Diffraction Standards*, Swarthmore, USA, 1997; [a]file 39-1425; [b]file 37-1484; [c]file 33-0111.
23. Denofre, S.; Gushikem, Y.; de Castro, S.C.; Kawano, Y.; *J. Chem. Soc., Faraday Trans*. **1993**, *89*, 1057.
24. Bhattacharyya, D.K.; Dutta, N.C.; *J. Nucl. Sci. Technol*. **1991**, *28*, 1014.
25. Parry, E.P.; *J. Catal*. **1963**, *2*, 371.
26. Morterra, C.; Cerrato, G.; *Langmuir* **1990**, *6*, 1810.
27. Zittel, H.E.; Florence, T. M.; *Anal. Chem*. **1967**, *39*, 320.
28. Benvenutti, E.V., Gushikem, Y.; Davanzo, C.U.; *Appl. Spectrosc*. **1992**, *46*, 1474.
29. Connel, G.; Dumesic, J.A.; *J. Catal*. **1987**, *105*, 285.
30. Lefrancois, M.; Malbois, G.; *J. Catal*. **1971,** *20*, 350.

Received: July 4, 2001
Published on the web: August 23, 2002

FAPESP helped in meeting the publication costs of this article.